

Possible Fluid Dynamical Interpretation of Some Reported Features in the Jovian Atmosphere

Abstract. Flow patterns of some of the features in the Voyager 1 imaging data for Jupiter appear to be consistent with those predicted by a solitary-wave theory.

We concentrate our attention on Jupiter's southern hemisphere and consider the two major types of disturbance found there. These features always occur together in space. They consist of a compact elliptically shaped formation, having an anticyclonic flow, poleward of a pair of more elongated cyclonic structures [already noted from Earth-based observations (1)]. The anticyclonic Great Red Spot (GRS) and the white ovals (WO's) and their associated cyclonic circulations are clear examples.

The cyclonic features that alternate with the chain of anticyclonic spots at 41°S are less elongated than those equatorward of the GRS and WO's because of the close longitudinal spacing of the anticyclones themselves. One may describe these by the cnoidal wave solutions to the appropriate nonlinear evolution equation. A further series of alternating anticyclonic and cyclonic regions

appears to exist at latitudes closer to the south pole, but the details are difficult to see because of the poor resolution in the published photographs. Some details of the flow fields around some of these features are given in Mitchell *et al.* (2), and the velocity distributions of the zonal jets are given in Ingersoll *et al.* (3). Further important velocity information can be reconstructed from figure 8 of Smith *et al.* (4) and a Jet Propulsion Laboratory movie sequence of cloud motions within the GRS.

In Fig. 1 we show a tracing from these sources of the motion of a cloud patch that shows a high-velocity jet around the periphery of the GRS with no penetration into the center and a very low velocity region in the spot's interior [also reported in (2)]. In Fig. 2 we show a result taken from (1) for the flow around a soli-

tary wave of the type that can exist in a zonal flow like that found in the Jovian atmosphere (5). The similarity to the observed flow fields around both the GRS and WO (Fig. 1) is striking. Such theoretical results have been produced for either a homogeneous or a stratified atmosphere.

The gross overall features are not expected to change dramatically when we extend the computations to atmospheric structure and zonal velocity profiles measured from Voyager infrared spectroscopy and radiometry (IRIS) data (6) and imaging data (3). These sources show that in the regions of interest $\beta < \delta^2 U / \delta y^2$ and that the Brunt frequency N is a function of altitude in the atmosphere (7). Under these circumstances, the appropriate extension of the solitary-wave theory presented in (1) [see also (8)] shows that, theoretically, we must consider a singular solitary-wave mode—one with a critical layer having $\beta \neq U''(y_c)$ at the latitude where $C_0 = U(y_c)$ (9) within the flow—and that the Korteweg-de Vries (KdV) equation is the first-order equation that is the most likely candidate to describe the east-west structure of the wave. Many of the details of such a wave have been worked out (8), and the internal flow structure associated with the wave is shown in Fig. 2c. In such flows and at high Reynolds numbers [$Re = U_0 L / \mu$, where U_0 is the typical jet velocity, about 50 m/sec; L is the scale of the feature, about 10^4 km for the GRS; and μ is the kinematic (eddy?) viscosity] the existence of a layer separating a low-velocity core from a high-speed outer flow is clear and the similarity between the flows shown in Figs. 1 and 2 is apparent. We recognize that a complete theory must also include a forcing term (an energy source) to balance the dissipation associated with the viscous layers shown here. It also should include the effect of vertical shear. Calculations including weak vertical shear have been performed (10). A forced wave demands a streamwise asymmetry in the dividing streamline and vertical shear introduces a latitudinal shift in the critical level as a function of altitude. There is no direct evidence of the latter effect, which indicates that the vertical shears are indeed weak.

This interpretation is also consistent in another respect. We know from Redekopp and Weidman (11) that for a model Jovian shear velocity profile $U = \pm U_0 \tanh y$, these waves, which evolve according to a KdV type of equation, are compact and elliptically shaped E-type waves in an anticyclonic shear and more elongated D-type waves in a cyclonic

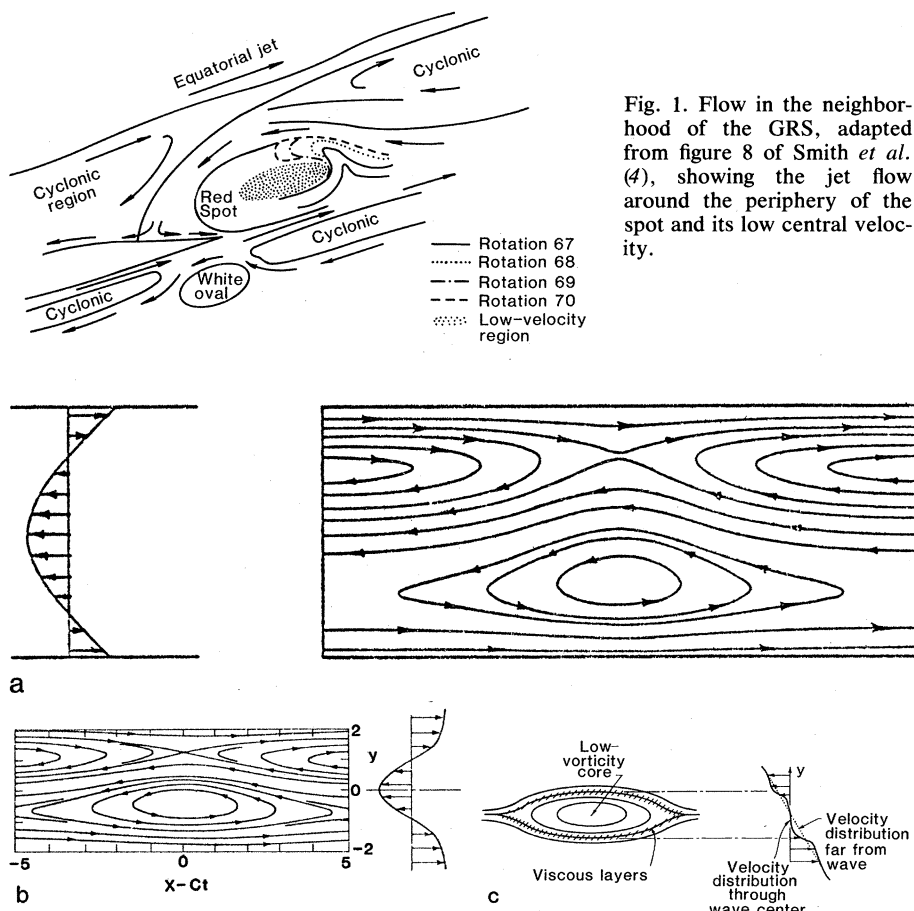


Fig. 2. Theoretical streamlines for (a) a barotropic flow bounded by latitudinal walls and (b) a stratified flow. These are combined D and E solitary waves, as discussed in (1). (c) Velocity distribution through the center of a solitary wave of elevation that contains a critical level. Viscous layers are required to smooth the profiles and the central velocity is low.

flow if their nondimensional phase speed is $-0.26 < C_0/U_0 < 0$. [The E waves are solitary waves of elevation and the D waves solitary waves of depression (1).] On the basis of the jet profiles in (3), the latter criterion appears to be satisfied for all the features under consideration—the GRS and WO's and the spots at 41°S as E waves and their surrounding cyclonic flows as D waves.

TONY MAXWORTHY

Departments of Mechanical and
Aerospace Engineering,
University of Southern California,
Los Angeles 90007,
and Planetary Atmospheres Section,
Jet Propulsion Laboratory,
Pasadena, California 91103

LARRY G. REDEKOPP

Department of Aerospace Engineering,
University of Southern California,
Los Angeles

References and Notes

1. T. Maxworthy and L. G. Redekopp, *Icarus* **29**, 261 (1979).
2. J. L. Mitchell *et al.*, *Nature (London)* **280**, 776 (1979).
3. A. P. Ingersoll *et al.*, *ibid.*, p. 773.
4. B. A. Smith *et al.*, *Science* **204**, 951 (1979).
5. We emphasize that the shape of the dividing streamline and the structure of the interior flow are determined theoretically for these waves with critical levels. The application to the GRS requires an extension of KdV theory to the highly nonlinear regime, but experience with shallow water waves suggests that this is not unjustified.
6. R. Hanel *et al.*, *Science* **204**, 972 (1979).
7. Here $U(y)$ is the variation of zonal velocity with north-south coordinate y and $\beta = 2\Omega \cos \theta/R$, where Ω and R are the planetary rotation rate and radius and θ is the latitude. The Brunt frequency $N = -g \log \rho / \delta z$, where g is the local gravitational acceleration and $\rho(z)$ is the variation of atmospheric density ρ with height z .
8. L. G. Redekopp, *J. Fluid Mech.* **82**, 725 (1977).
9. Here C_0 is the speed of long waves in the given shear and density profiles and is calculated as the eigenvalue of the associated north-south modal equation [see L. G. Redekopp (8)] and y_c is the critical latitude.
10. P. D. Weidman and L. G. Redekopp, *J. Atmos. Sci.*, in press.
11. L. G. Redekopp and P. D. Weidman, *ibid.* **35**, 790 (1978).

11 February 1980; revised 24 June 1980

Lightning on Jupiter: Rate, Energetics, and Effects

Abstract. *Voyager data on the optical and radio-frequency detection of lightning discharges in the atmosphere of Jupiter suggest a stroke rate significantly lower than on the earth. The efficiency of conversion of atmospheric convective energy flux into lightning is almost certainly less than on the earth, probably near 10^{-7} rather than the terrestrial value of 10^{-4} . At this level the rate of production of complex organic molecules by lightning and by thunder shock waves is negligible compared to the rates of known photochemical processes for forming colored inorganic solids.*

The Voyager imaging team (1) reported the detection of lightning-like flashes in nightside observations of Jupiter. Cook *et al.* (2) analyzed the spacecraft images in order to map the locations of these flashes onto the cloud features observed during daylight. Twenty flashes were identified in a time exposure of 192 seconds (2). The flashes were estimated to generate $\sim 10^{17}$ ergs "comparable to terrestrial superbolts" (1). Ordinary lightning discharges on the earth are very variable in strength, but typical discharges dissipate roughly 0.5×10^{16} to 1×10^{16} ergs (3). The field of view of the television image containing the lightning flashes extends from $\sim 30^\circ\text{N}$ to 80°N , with most coverage between longitudes 25°W and 75°W . Although the area covered is in excess of $2 \times 10^9 \text{ km}^2$, much of this is viewed at low grazing angles. All the observed flashes lie within an area of $\sim 1 \times 10^9 \text{ km}^2$, which is about twice the surface area of the entire earth. Flashes are observed up to 55°N , with 19 of 20 lying within the complex polar region ($> 45^\circ\text{N}$) (1).

The Voyager plasma-wave experiment (4) also reported evidence of lightning. While (and only while) the spacecraft was near 5.5 to 6.0 Jupiter radii (R_J) near

the equatorial plane, a number of frequency-dispersed radio impulses were detected with an event rate of about one in 8 seconds (5). These impulses are whistlers, similar to those formed by propagation of electromagnetic burst noise from terrestrial lightning discharges roughly along field lines in the magnetosphere (6). The whistler rate observed by Voyager is well within the range of rates observed on the earth at middle to high magnetic latitudes (6). The Voyager planetary radio astronomy experiment also searched for evidence of lightning, but the evidence has so far not been conclusive (7).

Further analyses of the plasma-wave experiment data (5, 8) have shown that these whistlers originate at high latitudes ($\sim 66^\circ\text{N}$, the foot of the field lines near which the whistlers were observed) and

follow paths which, aside from complications introduced by the high electron density in Io's plasma torus, roughly follow the magnetic lines of force in the relatively undistorted inner magnetosphere (near magnetic shell $L \approx 6$).

I will now make estimates of the frequency of occurrence of both optical flashes and radio-frequency whistler bursts and the associated energy dissipation rates.

The 20 flashes observed over 10^9 km^2 in 192 seconds amount to $3 \times 10^{-3} \text{ km}^{-2} \text{ year}^{-1}$, which, at 10^{17} ergs per discharge, gives $\sim 10^{-3} \text{ erg cm}^{-2} \text{ sec}^{-1}$. The convective energy flux averaged over Jupiter is $0.9 \times 10^4 \text{ erg cm}^{-2} \text{ sec}^{-1}$, so that the energy released by visible lightning flashes is $\sim 10^{-7}$ of the convective energy flux. I use here only the contribution to the atmospheric energy flux due to the turbulent upward transport of the internal heat of Jupiter, a conservative assumption applicable down to great depths in the troposphere (9). At pressures near 2 bars, deposition of solar heat can increase this figure by as much as a factor of ~ 2.5 at low latitudes, which, of course, would reduce the efficiency by the same factor.

The size of the area from which the plasma-wave experiment can detect lightning bursts is difficult to estimate precisely. Two effects contribute to the geographic spread of whistler signals. First, radio burst noise in the neutral atmosphere may be propagated for considerable distances, until it encounters an area where the critical frequency of the ionosphere is low and there passes through the ionosphere to initiate a whistler (10). Even low-altitude earth satellites can detect whistlers originating from discharges as far as 1000 km from the foot of the local field line (6, 11). Second, once a whistler originates in the ionosphere, it may propagate at a substantial angle with respect to the field lines (12). At frequencies very much less than the electron gyro frequency f_g (which was about 4.2 kHz at the point of whistler detection) the angle is about 19° ; it decreases to 11° at $0.19 f_g$ and rises to allow all directions at f_g (6), where the signal is strongly attenuated. Ray tracing (8) shows that noticeably different paths

Table 1. Energy available for disequilibrating processes on Jupiter.

Process	Principal products	Available flux ($\text{erg cm}^{-2} \text{ sec}^{-1}$)	Reference
CH_4 photolysis ($< 1600 \text{ \AA}$)	$\text{C}_2\text{H}_6, \text{C}_2\text{H}_2$	0.2	(15)
NH_3 photolysis ($< 2300 \text{ \AA}$)	$\text{N}_2, \text{N}_2\text{H}_4$	10	(16)
PH_3 photolysis ($< 2300 \text{ \AA}$)	P_4 (red)	15	(17)
H_2S photolysis ($< 2700 \text{ \AA}$)	S_x (yellow \rightarrow brown)	100	(18)
Lightning	$\text{CO}, \text{C}_2\text{H}_2, \text{HCN}$	< 0.003	(14)